ENERGY DISTRIBUTIONS IN ACTIVELY AND PASSIVELY CONTROLLED NONLINEAR STRUCTURES

A. YANIK[1], U. ALDEMIR[2] & M. BAKIOGLU[2]
[1]Department of Civil Engineering, Florida Institute of Technology, Melbourne, FL, USA.
[2]Department of Civil Engineering, Istanbul Technical University, Istanbul, Turkey.

ABSTRACT

In this study, the energy distributions of actively or passively controlled multistory nonlinear shear structures are investigated. Nonlinear differential equations of motion of the structure and the energy equations are derived for an uncontrolled and a controlled structure. A computer program which takes into account the nonlinearity of the material is developed and used for the dynamic analysis of the controlled and the uncontrolled structure. As numerical examples, two different structures are examined with six different control cases. These structures are a three-story and a twelve-story shear structure. In the dynamic analysis, the Erzincan and El Centro earthquakes are used. Active and passive controls are obtained by implementing base isolation and a mass damper into the structure. In addition, a hybrid structural control case is examined by implementing base isolation with an active mass damper to the structure. In total, six different passive and active control cases are investigated. An instantaneous optimal control algorithm, which minimizes the performance index defined as a time-dependent quadratic scalar functional instead of a quadratic integral functional and takes into account only the current state, is used as an active control algorithm. The results are given as force-displacement, acceleration, and energies in a comparative way for uncontrolled and controlled structures. The results show that the responses of the structure are reduced and the structural behavior is improved by using structural control.

Keywords: Active control, earthquake, energy, passive control, structural control.

1 INTRODUCTION

The idea of adapting structures to uncertain dynamic effects brought about the use of passive and active devices in civil engineering structures. Active control of structures was first investigated in the pioneering work by Yao [1]. Since then researchers have investigated active control for reducing the excessive vibration caused by strong winds and earthquakes. Besides active control, passive control devices have also been used in protecting structures from earthquake-induced vibrations. In actively controlled structures, control forces are generated by an external energy supply available in the system. External energy supplies are not required in passive systems. Passive control devices transform the input seismic energy into different forms. Hybrid control systems incorporate both active and passive devices.

The history of structural design can be categorized as classical, modern, and postmodern [2]. Static effects were taken into account in classical times, while dynamic effects were considered in the modern era. In recent years, feedback systems have been introduced to apply control forces.

Structural control is used in earthquake resistant designs and in very flexible structures. Recently, the strength of materials has not increased in proportion to their stiffness. Thus, the resulting structures with these new materials have become very flexible. Drift of the top floor of the World Trade Center, built with modern materials, was about 90 cm in severe winds, while it was about 7 cm for the Empire State Building, built with classical materials. Consequently, damage risk for windows and doors increases in flexible structures. Personal comfort is also a problem for occupants of high-rise buildings.

ISSN: 2046-0546 (paper format), ISSN: 2046-0554 (online), http://journals.witpress.com
DOI: 10.2495/CMEM-V2-N1-14-29

The aforementioned circumstances prompted researchers to investigate active control for reducing the excessive vibration caused by strong winds and earthquakes [3, 4]. There have been increasing developments to improve the performance of active controlled systems [5–7]. Besides active control, passive control devices have also been used in protecting structures from earthquake-induced vibrations [8–10]. The design of these systems takes into account the energy input; however, energy based earthquake resistant design is still a growing research area. In this type of design, the most important parameter is the amount of seismic energy input. As the amount of seismic energy input to a structure is decreased or diminished by control devices, the earthquake resistance of the structure increases. Some researchers have presented an active control algorithm using the probability density function of the structural energy [11]. The efficiency of a proposed algorithm is assessed in [12] by investigating control energies. State of the art techniques for energy dissipation in structures using active or passive devices is investigated in [13]. Some authors suggested that further research is needed to study the application of energy density on multi degree of freedom structures subjected to different earthquake ground motions in [14]. A method of generating energy density spectra obtained from earthquake response in actively controlled structural models is proposed for a practical application based on the definition of different energy forms in [15]; in this study, the authors also mentioned that research related to energy spectra is still limited and therefore more study should be carried out in order to gain a thorough understanding of the variation of different energy forms under earthquake excitation. A computational method is developed to characterize the energy in inelastic structures and the transfer among various energy forms over the duration of an earthquake in [16]. The investigation of the distribution of energies in an actively and passively controlled three-story structure is given in [17]. Maximum control energy dissipation is used to define the most effective optimal linear control law in [18]. Some energy-based active control algorithms are proposed in [19]. In order to simultaneously consider the mechanical energy of the structure, control and the seismic energies in the minimization procedure, a new performance index was proposed in [20].

The distribution of energy and the dynamic behavior of a structure with different active or passive control cases are studied in this paper. The material model is taken as bilinear elasto-plastic. Since the structural material is assumed to be bilinear, the corresponding problem is nonlinear. Two shear structures are investigated as an example problem. These structures are a three-story and a twelve-story structure. Five different cases of structural control are analyzed and compared with each other and with an uncontrolled structure. These cases are a structure with base isolation, a structure with a passive mass damper at the top of the building, a structure with an active mass damper at the top the building, a structure with base isolation and a passive mass damper at the base of the building, and a structure with base isolation and an active mass damper at the top of the building. Through these control cases, examples of passive, active and hybrid control systems in structures are investigated.

2 FORMULATION OF THE PROBLEM

The investigated shear building model is given for a structure with base isolation (Fig. 1a), with a passive mass damper or an active mass damper (Fig. 1b), with base isolation and a passive mass damper at the base of the building (Fig. 1c) and with base isolation and an active mass damper at the top of the building (Fig. 1d). The first two structures are passively controlled, the third structure (a structure with active mass damper) is an actively controlled structure, while the last system can be classified as a hybrid control system.

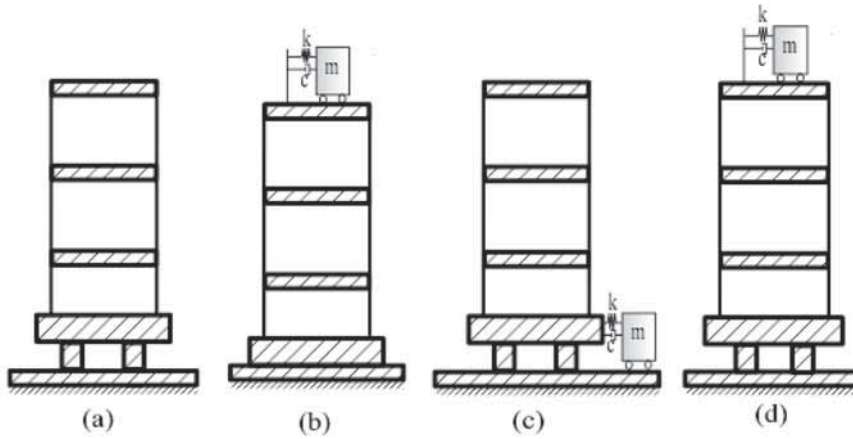

Figure 1: Structure with different control schemes.

For an inelastic shear building with n degrees of freedom under the influence of one dimensional ground motion and control forces, the equation of the motion of the structure can be written in matrix form as

$$\mathbf{M}\ddot{\mathbf{Y}}(t) + \mathbf{F}^d(t) + \mathbf{F}^k(t) = -\mathbf{M}\mathbf{V}\, f(t) + \mathbf{L}\mathbf{U}(t) \tag{1}$$

where $\ddot{\mathbf{Y}}(t) = (\ddot{y}_1, \ddot{y}_2, ..., \ddot{y}_n)^{\mathrm{T}}$ is the n-dimensional relative acceleration vector denoting the relative acceleration of each story unit; $\mathbf{M}$ is the $(n \times n)$-dimensional constant mass matrix with diagonal elements (m_i = mass of ith story, $i = 1,2,\ldots,n$); $\mathbf{F}^d$(t) and $\mathbf{F}^k$(t) are n-dimensional damping and stiffness force vectors respectively; $\mathbf{V} = (1,\ldots,1)^{\mathrm{T}}$ is the n-dimensional vector; $\mathbf{L}$ is the $(n \times r)$-dimensional location matrix of r controllers; $\mathbf{U}(t)$ is the r-dimensional active control force vector, and scalar function $f(t)$ is the one-dimensional earthquake acceleration. For the uncontrolled and passively controlled cases, the second term on the right-hand side of the equation becomes zero.

A wide variety of papers in the literature deals with relative acceleration responses. In this study the absolute acceleration responses of the uncontrolled and controlled structures are also investigated. The absolute acceleration response of a structure can be defined as:

$$\ddot{\mathbf{Y}}(t)_{abs} = \ddot{\mathbf{Y}}(t) + \mathbf{V}f(t) \tag{2}$$

Introducing a $2n$-dimensional state vector, $\mathbf{Z}(t)$, as follows:

$$\mathbf{Z}(t) = \begin{bmatrix} \mathbf{Y}(t) \\ \dot{\mathbf{Y}}(t) \end{bmatrix} \tag{3}$$

the second-order matrix equation of motion can also be rewritten as a first order matrix equation with dimension $2n$ in the following form:

$$\dot{\mathbf{Z}}(t) = \mathbf{A}\mathbf{Z}(t) + \mathbf{B}\mathbf{U}(t) + \mathbf{H}f(t) \qquad \mathbf{Z}(0) = \mathbf{Z}_0 \tag{4}$$

where

$$\mathbf{A} = \begin{bmatrix} \mathbf{0} & \mathbf{I} \\ -\mathbf{M}^{-1}\mathbf{K} & -\mathbf{M}^{-1}\mathbf{C} \end{bmatrix} \quad \mathbf{B} = \begin{bmatrix} \mathbf{0} \\ \mathbf{M}^{-1}\mathbf{L} \end{bmatrix} \quad \mathbf{H} = \begin{bmatrix} \mathbf{0} \\ -\mathbf{V} \end{bmatrix} \tag{5}$$

In eqn (5), **I** is an $(n \times n)$-dimensional identity matrix, **K** is the $(n \times n)$-dimensional stiffness matrix, and **C** is the $(n \times n)$-dimensional viscous damping matrix. Material nonlinear behavior is defined for this structure. The nonlinearity of the model has been defined by changing the stiffness matrix **K**. If the structural strains exceed a limit value, the stiffness of the structure is reduced by multiplying **K** by 0.1. The bilinear hysteresis model is given in (Fig. 2) [21].

To obtain the control force $\mathbf{U}(t)$ in eqn (4), a control algorithm must be chosen. After defining the control force, eqn (4) can be solved. In this study, the instantaneous optimal control algorithm, which minimizes the performance index defined as a time-dependent quadratic scalar function, is used instead of a quadratic integral function and takes into account only the current state.

2.1 Instantaneous optimal control algorithm

Most studies in the literature are based on the classical linear optimal control algorithm (linear-quadratic regulator or LQR). In LQR control, the nonlinear matrix Riccati equation is obtained by ignoring the earthquake excitation term, so classical closed-loop control is approximately optimal. Although classical open-loop and closed open-loop control are superior to classical closed-loop control, they require knowledge of the whole history of earthquake excitations, and therefore, they cannot be applied to real structures. This closed loop algorithm can compute control forces only for a given earthquake excitation. A real time computation of the control forces under a real earthquake excitation with this algorithm is not possible. To overcome this difficulty, the instantaneous control algorithm, which minimizes the performance index defined as a time-dependent quadratic scalar function instead of as a quadratic integral function and takes into account only the current state, was proposed by Yang *et al.* [22]. In this control algorithm, the time-dependent performance measure, which will be minimized, can be expressed as

$$J = \mathbf{Z}^{\mathrm{T}}(t)\mathbf{Q}\,\mathbf{Z}(t) + \mathbf{U}^{\mathrm{T}}(t)\mathbf{R}\mathbf{U}(t) \quad \rightarrow \quad \min \tag{6}$$

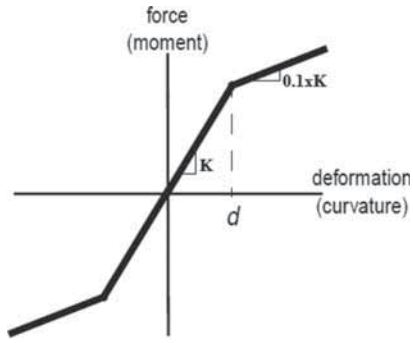

Figure 2: Bilinear hysteresis model.

In eqn (6), **Q** is a ($2n \times 2n$)-dimensional positive semi-definite symmetric weighting matrix, and **R** is a ($r \times r$)-dimensional positive-definite symmetric weighting matrix. The values of **Q** and **R** matrices are assigned according to the relative importance of the state variables and the control forces in the minimization procedure. If the elements of the matrix **Q** are chosen larger than the elements of **R**, minimizing the response of the structure is more important than the control forces; otherwise, minimization of the control forces is more important. The resulting optimal control law and the state vector can be obtained as

$$\mathbf{U}^* = -\frac{\Delta t}{2}\mathbf{R}^{-1}\mathbf{B}^{\mathrm{T}}\mathbf{Q}\mathbf{Z}^*(t) \tag{7}$$

$$\mathbf{Z}^* = [\mathbf{I} + \frac{(\Delta t)^2}{4}\mathbf{B}\mathbf{R}^{-1}\mathbf{B}^{\mathrm{T}}\mathbf{Q}]^{-1}[\mathbf{T}\mathbf{D}(t-\Delta t) + \frac{\Delta t}{2}\mathbf{H}f(t)] \tag{8}$$

The detailed derivation of eqns (7) and (8) can be found in Yang *et al.* [22].

3 ENERGY EQUATIONS

For an actively controlled structure, if eqn (1) is multiplied with the transpose of the velocity vector $\mathrm{Y}^{\mathrm{T}}(t)$ and integrated in the interval of (0–t), the energy equations will be obtained and expressed as

$$\begin{aligned}\int_0^t \dot{\mathbf{Y}}^{\mathrm{T}}(\tau)\mathbf{M}\ddot{\mathbf{Y}}(\tau)d\tau + \int_0^t \dot{\mathbf{Y}}^{\mathrm{T}}(\tau)\mathbf{F}^d(\tau)d\tau + \int_0^t \dot{\mathbf{Y}}^{\mathrm{T}}(\tau)\mathbf{F}^k(\tau)d\tau \\ = -\int_0^t \dot{\mathbf{Y}}^{\mathrm{T}}(\tau)\mathbf{M}\mathbf{V}\ddot{x}_0 d\tau + \int_0^t \dot{\mathbf{Y}}^{\mathrm{T}}(\tau)\mathbf{L}\mathbf{U}d\tau\end{aligned} \tag{9}$$

The first term on the left hand side of eqn (9) is called kinetic energy (E_{kin}) and can be written as

$$E_{kin} = \int_0^t \dot{\mathbf{Y}}^{\mathrm{T}}(\tau)\mathbf{M}\ddot{\mathbf{Y}}(\tau)d\tau = \int_0^t \frac{d}{dt}[\dot{\mathbf{Y}}^{\mathrm{T}}(\tau)\mathbf{M}\dot{\mathbf{Y}}(\tau)]d\tau = \frac{1}{2}\dot{\mathbf{Y}}^{\mathrm{T}}(t)\mathbf{M}\dot{\mathbf{Y}}(t) \tag{10}$$

E_{kin} is sum of the kinetic energy of all masses with respect to the ground. In eqn (9) the second term on the left hand side is equal to the damping energy of the system, E_{damp}, which can be expressed as

$$E_{damp} = \int_0^t \dot{\mathbf{Y}}^{\mathrm{T}}(\tau)\mathbf{F}^k(\tau)d\tau \tag{11}$$

The third term on the left hand side of eqn (9) is the strain energy E_{str}, which can be written as

$$E_{str} = \int_0^t \dot{\mathbf{Y}}^{\mathrm{T}}(\tau)\mathbf{F}^k(\tau)d\tau \tag{12}$$

If the system is linear elastic $\mathbf{F}^k = \mathbf{K}\mathbf{Y}$, the third term in eqn (9) for the linear elastic case can be expressed as

$$E_{str}^{elas} = \int_0^t \dot{\mathbf{Y}}^{\mathrm{T}}(\tau)\mathbf{K}\mathbf{Y}(\tau)d\tau = \frac{1}{2}\mathbf{Y}^{\mathrm{T}}(t)\mathbf{K}\mathbf{Y}(t) \tag{13}$$

Equation (13) is valid if the system is totally elastic. If the strains of the system exceed the elastic limit, strain energy can be divided to two types, one of which is recovered elastic energy and the other of which is dissipated hysteretic energy. For this case, the total strain energy can be expressed as the total of the two types of energy

$$E_{str} = E_{str}^{elas} + E_{str}^{his} \tag{14}$$

The first term on the right hand side of eqn (9) is the earthquake energy of the structure E_{earth} and the last term is the control energy E_{con}; these energies can be expressed as

$$E_{earth} = -\int_0^t \dot{\mathbf{Y}}^{\mathrm{T}}(\tau)\mathbf{M}\mathbf{V}\ddot{x}_0 d\tau \quad ; \quad E_{con} = \int_0^t \dot{\mathbf{Y}}^{\mathrm{T}}(\tau)\mathbf{L}\mathbf{U}\, d\tau \tag{15}$$

If we move E_{con} in eqn (15) to the left hand side of eqn (9), it will have a negative sign in front of it. Although it has a negative sign, it is positive because control forces generally depend negatively on displacement and velocity response, so this makes the control energy positive. After defining this, the energy equilibrium can be expressed as

$$E_{kin} + E_{damp} + E_{str}^{elas} + E_{str}^{his} + E_{con} = E_{earth} \tag{16}$$

Equation (16) shows that applying control force can dissipate energy when the control force is applied in the direction opposite to the displacement and velocity responses, as with other forms of energy. This indicates that control elements are a kind of energy dissipating mechanism like damping in the structures.

4 NUMERICAL EXAMPLES

As an example problem, a three-story (S1) [17] and a twelve-story (S2) shear building with damping are considered under the effect of two different earthquake motions, which represent the El Centro and Erzincan earthquakes. These two earthquakes have been chosen to give a more general conclusion for the behavior of the structure. The El Centro NS (1940) earthquake excitation had a peak ground acceleration of $0.34\,g$ and can be classified as a moderate earthquake, where Erzincan NS (1995;95 Erzincan station) had a peak of $0.41\,g$ and can be classified as a strong earthquake (g is the gravitational acceleration). Acceleration time histories of the El Centro and the Erzincan earthquakes are given in Fig. 3. The columns of the building are assumed as massless, and the mass of the structure is concentrated at the floor level as a lumped mass model. Each story has the same mass, stiffness, and damping parameters for the three-story building. As control elements, base isolation and mass damper are chosen.

The dynamic behavior of these structures are investigated for six cases which are an uncontrolled case (C1), a structure with base isolation (C2), a structure with base isolation and a passive mass damper (C3), a structure with base isolation and an active mass damper (C4), a structure with a passive mass damper (C5), and a structure with an active mass damper (C6). For both structures, the weighting matrix $\mathbf{R}$ (1×1) is chosen as 10^{-4}, a scalar number, because only a single active mass damper is in the system for the active control case (C4). The other weighting matrix $\mathbf{Q}$ is chosen as (10×10) diagonal matrix of the diagonal elements which

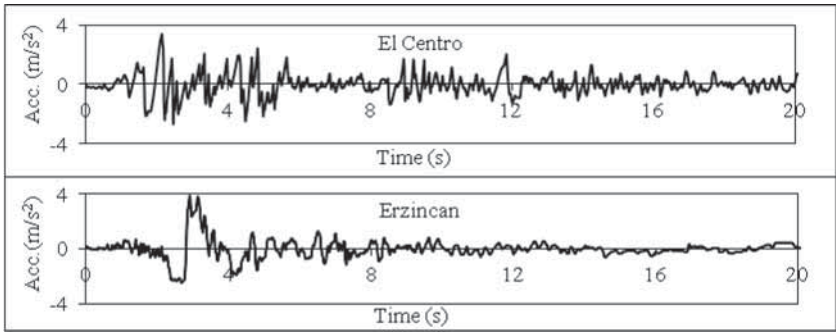

Figure 3: Earthquake time history.

consist of 1000 for the three-story structure, while a (28 × 28) diagonal matrix with 1000 diagonal elements is used for the twelve-story structure. For the active control case (C6), **R** (1 × 1) is chosen as 10^{-5} for both structures. The **Q** matrix is chosen to be an (8 × 8) diagonal matrix with diagonal elements which consist of 10000 for the three-story structure; for the twelve-story structure it is chosen to be a (26 × 26) diagonal matrix with diagonal elements equal to 10000.

The **Q** and **R** matrices must be positive-definite and positive semi-definite matrices, respectively. The values of the elements of these matrices satisfy these conditions. Unfortunately, there are no systematic approaches or exact rules in general on how to assign the values of the weighting matrices. The tuning of the weighting matrices reflects the trade-off between the desired performance and control energy consumption, and it provides the designer with significant flexibility. However, within the framework of this study, these weighting matrices are required to guarantee the stability of the controlled structure.

4.1 Three-story structure (S1)

The mass, stiffness, and damping parameters of the base isolation are m_b = 100 tons, k_b = 2527 × 10^3 kN/m and c_b = 63 kNs/m, respectively. For the passive and active mass damper the respective parameters are m_d = 36.3 tons, k_d = 1173 kN/m, and c_d = 31 kNs/m. The mass, stiffness, and damping matrices of the structure for the uncontrolled case are as follows:

$$\mathbf{M} = \begin{bmatrix} 100 & 0 & 0 \\ 0 & 100 & 0 \\ 0 & 0 & 100 \end{bmatrix} \text{ton}, \quad \mathbf{C} = \begin{bmatrix} 251.32 & -125.66 & 0 \\ -125.66 & 251.32 & -125.66 \\ 0 & -125.66 & 125.66 \end{bmatrix} \text{kNs/m}$$
$$\mathbf{K} = \begin{bmatrix} 31582.734 & -15791.34 & 0 \\ -15791.34 & 31582.734 & -15791.34 \\ 0 & -15791.34 & 15791.34 \end{bmatrix} \text{kN/m} \tag{17}$$

The percentage of the maximum uncontrolled displacement reduction of the stories is given in Table 1 for S1. The maximum displacements of the base isolation and mass damper are given in Table 2. It can be seen from Table 1 that among all cases the largest reduction in the story displacements has been obtained for the hybrid system, which consists of an active

Table 1: Uncontrolled response reduction percentages (%).

		Control cases				
Earthquake	Story No.	C2	C3	C4	C5	C6
El Centro	1	–26.3	11.6	17.6	19.0	15.8
	2	70.4	73.1	73.6	40.4	43.9
	3	83.7	85.5	83.7	70.7	72.8
Erzincan	1	3.6	–7.7	14.6	6.8	13.6
	2	38.8	27.5	45.5	33.7	47.4
	3	91.6	90.5	91.9	89.2	92.6

Table 2: Maximum responses of the control elements (m).

		Control cases				
Earthquake	Control elements	C2	C3	C4	C5	C6
El Centro	Mass damper	-	0.0649	0.0516	0.1737	0.1221
	Base isolation	0.2039	0.2144	0.1868	-	-
Erzincan	Mass damper	-	0.1401	0.1491	0.5454	0.4528
	Base isolation	0.3306	0.3649	0.341	-	-

mass damper and base isolation (C4). An active mass damper has also reduced the displacement of the base isolation. Implementing a passive mass damper to the structure with base isolation has also reduced the story displacements for the El Centro earthquake. For the single active mass damper case (C6), the displacement of the mass damper is significantly smaller than in the single passive mass damper case (C5). In addition, the story displacements are smaller for the single active mass damper case than for the single passive mass damper case. Table 2 also indicates that for the single mass damper cases (C5, C6), the displacement of the mass damper is larger than for hybrid cases (C3), (C4). Moreover, implementing base isolation to the uncontrolled structure has reduced the displacements. Within the control cases, the least effective one is the structure with a single passive mass damper (C5).

The hysteretic curves for the second story S1 under the El Centro earthquake are given in Fig. 4 for all cases. In Fig. 4, (C1) to (C6) represent the control cases defined above. Implementing base isolation to the system makes the structural behavior elastic for the El Centro earthquake for the (C2), (C3) and (C4) cases, but for the single passive mass damper (C5) and single active mass damper (C6) case the behavior is plastic. The behavior of the structure is similar for cases (C2), (C3) and (C4). Among single mass damper cases (C5, C6), the area covered by the hysteretic loops in the single active mass damper case is smaller than in the uncontrolled and passive mass damper case. Under the Erzincan earthquake, the hysteretic curves are given for the third story of the structure in Fig. 5. The behavior is elastic only for the structure with base isolation and an active mass damper, but for the single active controller case the behavior is very close to the totally elastic behavior.

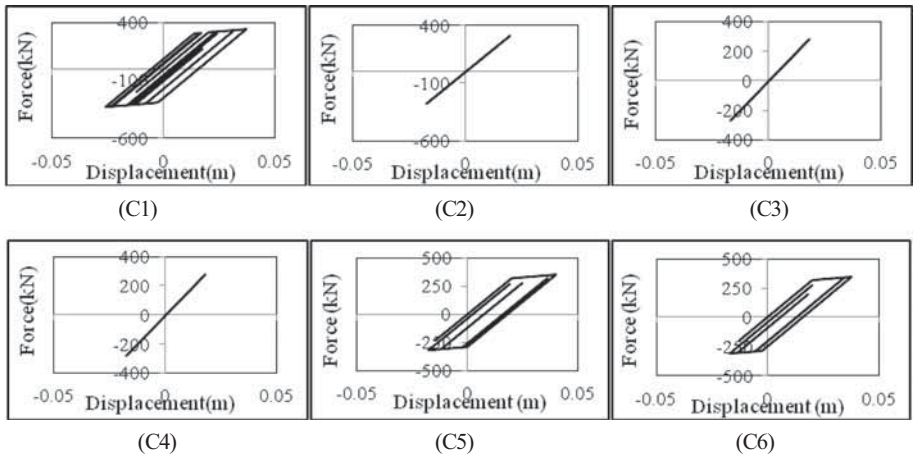

Figure 4: Hysteretic curves for El Centro earthquake.

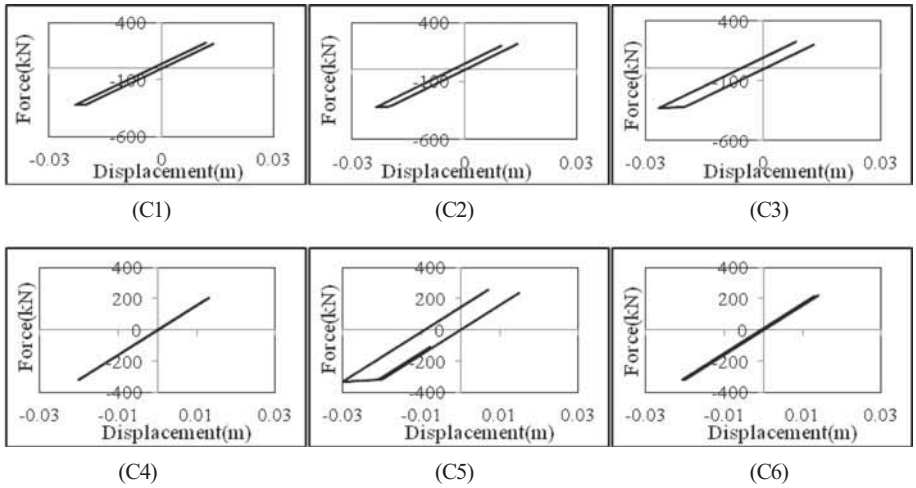

Figure 5: Hysteretic curves for Erzincan earthquake.

In addition to the displacement responses, the relative acceleration responses of the stories are given in Table 3. Table 3 indicates that implementing passive and active control devices to the structure significantly reduced the uncontrolled story relative accelerations except for the structure under the Erzincan earthquake. Especially, the uncontrolled relative accelerations of the second and third story are significantly reduced by implementing control devices to the structure. For the El Centro earthquake, the relative accelerations are reduced to the same extent for the three different control cases (C2, C3, and C4). For the single passive mass damper case, the accelerations are similar to those in an uncontrolled structure. For the Erzincan earthquake, implementing structural control elements increased the relative acceleration responses.

The absolute acceleration responses are given in Table 4. Implementing control elements to the structure has also reduced the absolute acceleration responses of all stories except for the first story under the Erzincan earthquake.

Table 3: Maximum relative accelerations of the stories (m/s^2).

		Control cases					
Earthquake	Story No.	C1	C2	C3	C4	C5	C6
El Centro	1	3.56	3.39	3.69	3.64	4.14	3.60
	2	5.33	3.67	3.58	3.48	5.00	4.81
	3	5.05	3.70	3.66	3.63	5.02	4.96
Erzincan	1	5.66	6.29	6.16	6.32	5.64	5.02
	2	5.84	5.76	5.60	6.03	5.44	5.68
	3	5.39	5.90	5.79	5.68	5.39	5.78

Table 4: Maximum absolute accelerations of the stories (m/s^2).

		Control cases					
Earthquake	Story No.	C1	C2	C3	C4	C5	C6
El Centro	1	2.12	1.52	1.41	1.55	2.10	1.77
	2	2.09	1.44	1.32	1.49	2.14	1.68
	3	2.99	1.72	1.54	1.32	2.89	2.73
Erzincan	1	3.00	3.65	3.49	3.36	3.66	2.73
	2	3.27	3.23	3.12	3.33	2.59	2.52
	3	3.34	3.26	3.28	2.90	3.38	3.04

It is known that the sum of the kinetic energy, the damping energy, the strain energy, and the control energy is equal to the earthquake energy. For passive control cases, the control energy is zero for the whole earthquake's duration. In addition, the increase in the control forces results in the increase in the control energy consumption.

For the uncontrolled, passive and active control cases, energy distributions are given in Fig. 6 for the El Centro earthquake. For the El Centro earthquake, the largest reduction in the strain energy has been obtained for the hybrid system, while the maximum control energy for this system is 29.11 kNm. In Fig. 6 it can be seen that the strain energy oscillates between 70 kNm and 92 kNm. This is because of the elasto-plastic behavior of the structure under the El Centro earthquake. The energy distributions for the Erzincan earthquake are given in Fig. 7. Under the Erzincan earthquake for the active control case, the maximum control energy is 38.15 kNm.

For two different earthquakes, implementing base isolation and mass damper to the structure has increased the total energy consumption of the structure.

4.2 Twelve-story structure (S2)

The dynamic behavior of a twelve-story structure is analyzed under the effect of the El Centro and Erzincan earthquakes. The same control cases are investigated. For the twelve-story structure, the structural parameters are given in Table 5.

The hysteretic curves for the first story of S2 under the El Centro earthquake are given in Fig. 8. Implementing base isolation to the system reduced the force and displacement

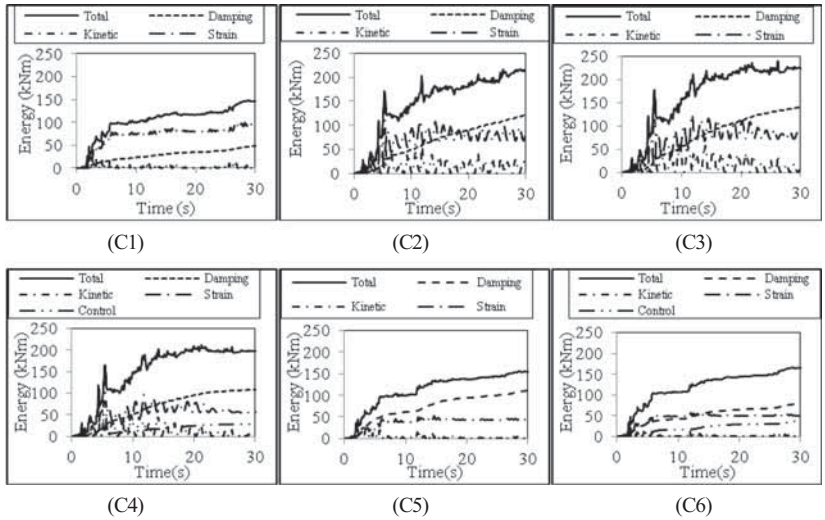

Figure 6: Seismic energy distributions for El Centro earthquake.

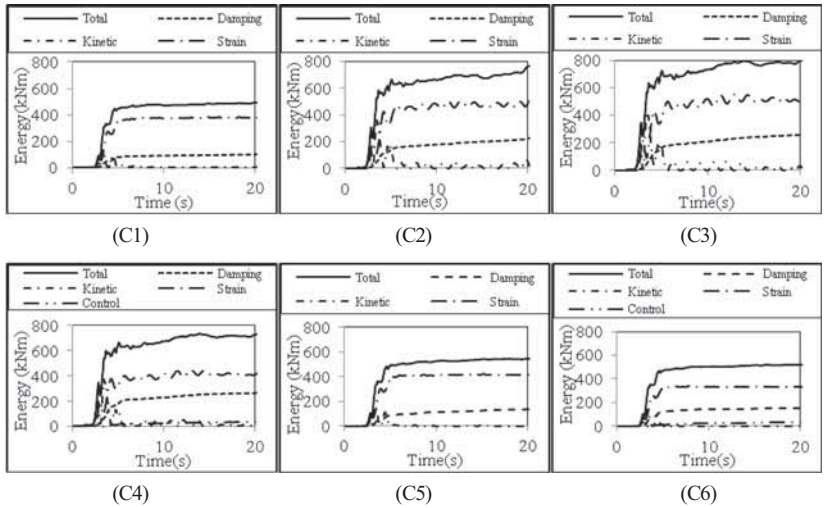

Figure 7: Seismic energy distributions for Erzincan earthquake.

Table 5: Structural parameters S2.

Story number and supplemental elements	Mass (tons)	Stiffness (k_1) (kN/m)	Damping (kNs/m)	Yielding level (cm)
1–11	500	500000	4952	2.5
12	300	500000	4952	2.5
Base isolation	500	20000	605	2.5
Mass damper (at the base)	500	1940.5	197	200
Mass damper (at the top)	100	1577	394	200

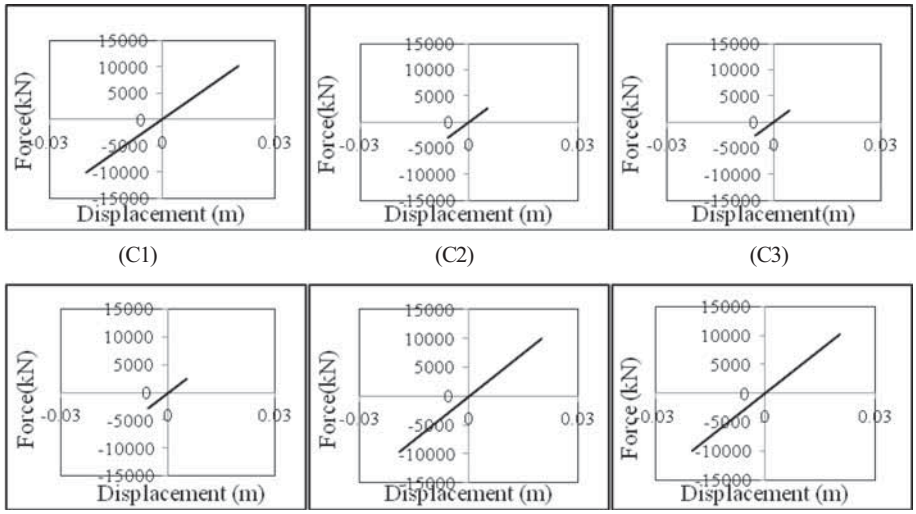

Figure 8: Hysteretic curve for El Centro earthquake.

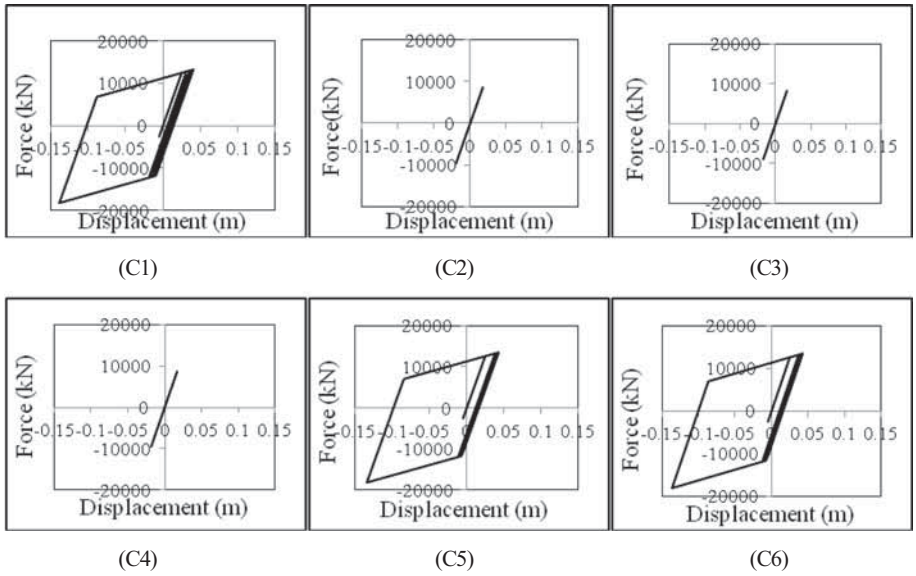

Figure 9: Hysteretic curves for Erzincan earthquake.

responses of the structure significantly. Under the effect of the Erzincan earthquake, the hysteretic curves for the first story of S2 are given in Fig. 9. Displacement of all of the stories is investigated and the most critical story has been determined to be the first story. Implementing base isolation to the structure makes the behavior elastic for the circumstances of the Erzincan earthquake for cases (C2), (C3) and (C4). The behavior is plastic for the single

passive (C5) and the single active mass damper case (C6). Cases (C2), (C3), and (C4) are equally effective in reducing the uncontrolled structural responses.

For the uncontrolled, passive and active control cases, maximum energy responses of the uncontrolled and controlled structures are given in Table 6. Table 6 indicates that the uncontrolled total, damping, kinetic, and strain energy have been reduced significantly for the controlled cases except in the single active and passive mass damper case for both earthquakes. The energies are approximately 1/3 of the uncontrolled structure energies for the El Centro earthquake. Table 6 also indicates that the maximum reduction for the uncontrolled energies has been obtained for damping energy by implementing structural elements. On the other hand, control energy consumption is very small in comparison with the other energy types. Control energy is between 1% and 2% of the total energy for both earthquakes. For the single passive and active mass damper case, the maximum values of the energies are approximately the same as with the uncontrolled structure. Moreover, for these two cases the control energies are higher than the structure with base isolation and active mass damper. In addition, the total energy is the smallest for the fourth case, which is the base isolation with active mass damper case for both earthquakes.

The increase in the strain energy causes multistructural damage. The structure can collapse because of a dramatic increase in strain energy. Distribution of the strain energy to the stories and supplemental elements has also been investigated in this study. If most of the strain energy is absorbed by the control elements, then this has a positive effect for a structure.

The distribution of the strain energy for the twelve-story structure during the Erzincan earthquake is given in Fig. 10. In Fig. 10, TSE represents the total strain energy of the structure, BI represents the base isolation, MD the mass damper, and the numbers 1, 6, and 12 represent the corresponding stories. Figure 10 indicates that for the uncontrolled case (C1), most of the strain energy is absorbed by the first floor, while the strain energy absorption decreases for the upper stories. It can be seen from Fig. 10 that base isolation absorbs the

Table 6: Maximum energy responses (S2).

Earthquakes	Control cases	Energies (kN-m)				
		Total	Damping	Kinetic	Strain	Control
El Centro	C1	2135.3	1846.4	1066.5	754.9	-
	C2	945.3	210.9	843.5	269.2	-
	C3	896.1	341.4	781.0	213.2	-
	C4	832.8	225.6	832.8	259.5	9.2
	C5	2023.6	1828.8	729.4	659.2	-
	C6	2119.5	1725.9	866.1	694.6	83.8
Erzincan	C1	13171.3	3425.7	4484.1	10093.3	-
	C2	5877.1	2155.5	5382.3	3003.3	-
	C3	5925.4	2764.7	5182.1	2541.5	-
	C4	5874.5	2192.3	5361.3	2948.0	74.3
	C5	13001.6	4057.9	4574.4	9690.5	-
	C6	13162.0	3587.1	4559.4	9966.7	204.0

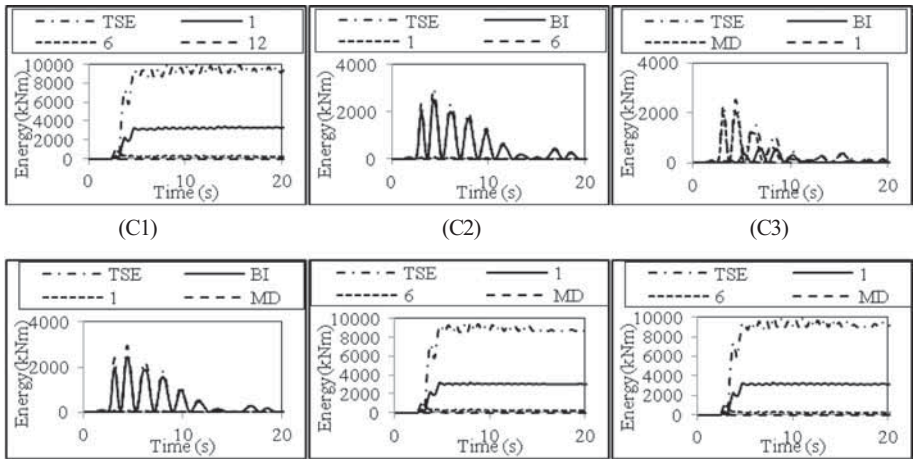

Figure 10: Distribution of strain energy for Erzincan earthquake.

great majority of the strain energy for (C2), (C3) and (C4) cases. Implementing base isolation to the structure decreases the total strain energy significantly as indicated from cases (C2), (C3) and (C4). In the sıngle passive or active mass damper cases (C5) and (C6), the total strain energy of the uncontrolled structure was not decreased. Implementing base isolation to the structure not only decreased the total strain energy consumption but also enabled the base to absorb the great majority of the total strain energy of the structure.

5 CONCLUSION

In the area of earthquake resistant structural design, there is a basic methodology. This methodology involves guaranteeing earthquake resistance by modifying structural form, for example, by decreasing the column rigidities (flexible ground floor) and by using hinged columns. The aim of this methodology is to diminish the seismic energy of a structure during earthquakes by providing various structural elements like columns to absorb this energy. The methodology investigated in this study involved achieving the decrease in seismic energy by implementing supplemental elements to a structure. By the detailed analysis of energy distributions of actively or passively controlled structures, it has been shown that applying control to the structures significantly reduces the energies within the structure. The other conclusions drawn from this study are given below.

- The earthquake characteristics mostly had effect on the energies of both controlled and uncontrolled structures. The same structures under the Erzincan earthquake, which had a higher peak acceleration than the El Centro earthquake, consumed dramatically more energies than in the El Centro earthquake.
- Weighting matrix **R** had an important effect on control energy consumption. The assignment of small values to this matrix resulted in small control energy consumption. The control energy consumption was very much lower than other types of structural energies.
- With respect to the analysis of the strain energy distribution of the stories, it has been determined that the maximum strain energy is dissipated by the first story, and the dissipation is reduced for the upper stories of the structure.

All of the above conclusions show the effectiveness of the control systems from an energy perspective. In addition, if the control elements are designed by increasing their energy dissipation capacities, more effective control systems can be produced.

ACKNOWLEDGEMENT

The authors gratefully acknowledge the support from the National and Technological Research Council of Turkey (TUBITAK) (Project No: 108M496). Any opinions and conclusions are those of the authors and do not necessarily reflect the views of the supporter.

REFERENCES

[1] Yao, J.T.P., Concept of structural control. *Journal of Structural Division ASCE*, **98**, pp. 1567–1574, 1972.

[2] Housner, G.W., Bergman, L.A., Caughey, T.K., Chassiakos, A.G., Claus, R.O., Masri, S.F., Skelton, R.E., Soong, T.T., Spencer, B.F. & Yao, J.T.P., Structural control: past, present, and future. *Journal of Engineering Mechanics ASCE*, **123(2)**, pp. 897–958, 1997.

[3] Aldemir, U., A simple active control algorithm for earthquake excited structures. *Computer-Aided Civil and Infrastructure Engineering*, **25**, pp. 218–225, 2010.

[4] Ramallo, J.C., Johnson, E.A. & Spencer, B.F., Smart base isolation systems. *Journal of Engineering Mechanics (ASCE)*, **128(10)**, pp. 1088–1099, 2002.

[5] Aldemir, U., Bakioglu, M. & Akhiev, S.S., Optimal control of linear buildings under seismic excitations. *Earthquake Engineering and Structural Dynamics*, **30**, pp. 835–851, 2001.

[6] Aldemir, U. & Bakioglu, M., Active structural control based on prediction and degree of stability. *Journal of Sound and Vibration,* **247(4)**, pp. 561–576, 2001.

[7] Aldemir, U., Predictive suboptimal semiactive control of earthquake response. *Structural Control and Health Monitoring*, **17,** pp. 654–674, 2010.

[8] Cimellaro, G.P., Lavan, O. & Reinhorn, A.M., Design of passive systems for control of inelastic structures. *Earthquake Engineering and Structural Dynamics*, **38**, pp. 783–804, 2009.

[9] Konar, T. & Ghosh, A., Passive control of seismically excited structures by the liquid column vibration absorber. *Structural Engineering and Mechanics*, **36(5)**, pp. 561–573, 2010.

[10] He, W.L. & Agrawal, A.K. Passive and hybrid control systems for seismic protection of a benchmark cable-stayed bridge. *Structural Control and Health Monitoring*, **14**, pp. 1–26, 2007.

[11] Wong, K.K.F. & Wang, Y. Probabilistic structural damage assessment and control based on energy approach. *The Structural Design of Tall Buildings*, **10**, pp. 283–308, 2001.

[12] Wong, K.K.F., Structural control energy efficiency based on elastic displacement. *Solid Mechanics and ıts Applications*, **130**, pp. 365–374, 2005.

[13] Soong, T.T. & Spencer, B.F., Jr., Supplemental energy dissipation: state-of-the-art and state-of-the-practice. *Engineering Structures*, **24**, pp. 243–259, 2002.

[14] Wong, K.K.F. & Zhao, D., Effectiveness of inelastic structural control based on elastic displacement and energy. *Structural Control and Health Monitoring*, **12**, pp. 47–64, 2005.

[15] Wong, K.K.F. & Pang, M., Energy density spectra in actively controlled inelastic structures-theory. *Structural Control and Health Monitoring*, **14**, pp. 261–278, 2007.

[16] Wong, K.K.F. & Yang, R., Evaluation of response and energy in actively controlled structures. *Earthquake Engineering and Structural Dynamics*, **30**, 1495–1510, 2001.

[17] Yanik, A., Aldemir, U. & Bakioglu, M., Energy-based evaluation of seismic response of structures with passive and active systems. *Proc. of the Earthquake Resistant Engineering Structures VIII*, eds. C.A. Brebbia & M. Magueri, **120**, pp. 67–78, 2011.

[18] Wong, K.K.F. & Yang, R., Effectiveness of structural control based on control energy perspectives. *Earthquake Engineering and Structural Dynamics*, **30**, pp. 1747–1768, 2001. doi: http://dx.doi.org/10.1002/eqe.76

[19] Lu, L.Y., Lin, G.L. & Lin, C.C., Absolute-energy-based active control strategies for linear seismic isolation systems. *Structural Control and Health Monitoring*, **18(3)**, pp. 321–340, 2011. doi: http://dx.doi.org/10.1002/stc.373

[20] Aldemir, U., Yanik, A. & Bakioglu, M., Control of structural response under earthquake excitation. *Computer-Aided Civil and Infrastructure Engineering*, **27(8)**, pp. 620–638, 2012. doi: http://dx.doi.org/10.1111/j.1467-8667.2012.00776.x

[21] Ohtori, Y., Christenson, R.E., Spencer, B.F., Jr. & Dyke, S.J., Benchmark control problems for seismically excited nonlinear buildings. *Journal of Engineering Mechanics*, **130(4)**, pp. 366–385, 2004. doi: http://dx.doi.org/10.1061/(ASCE)0733-9399(2004)130:4(366)

[22] Yang, J.N., Akbarpour, A. & Ghaemmaghami, P., New optimal control algorithms for structural control. *Journal of Engineering Mechanics ASME*, **113(9)**, pp. 1369–1386, 1987. doi: http://dx.doi.org/10.1061/(ASCE)0733-9399(1987)113:9(1369)